

On study of X-ray absorption and properties of dispersion of W, MoS₂ and B₄C particles in high density polyethylene

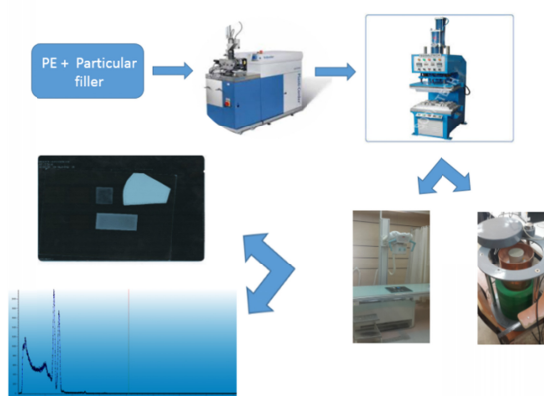
Maryam Afshar, Jalil Morshedian*, Shervin Ahmadi

Department of Polymer Processing, Iran Polymer and Petrochemical Institute, Tehran, Iran

HIGHLIGHT

- 45% (wt) tungsten powder dispersed in HDPE has a comparable x-ray shielding performance to lead.
- This developed composite material also has γ -ray radiation attenuation capability with no degradation in its polymer matrix.
- The highly W filled material has the same processability as its neat polymer constituent.
- Enhancement of yield stress and strength of HDPE with W loading imparts better load bearing performance.

GRAPHICAL ABSTRACT



ARTICLE INFO

Article history:

Received 25 January 2017

Revised 04 July 2017

Accepted 23 September 2017

Keywords:

Radiation attenuation

Dispersion rheology

Metallic compounds

Radiology

X-ray

Gamma-ray

ABSTRACT

Shielding radiation from both x-rays and gamma-rays is important for personnel in medical fields e.g. interventional radiology, nuclear power stations, and other inspection facilities where radiation is involved. Lead is known for its effective shielding property against these high energy radiations, however heaviness and toxicity are its main drawback. In this study effectiveness of non-lead polymeric composite materials, which include high-atomic-number / or known barrier elements to absorb photons from the radiations was evaluated. High density polyethylene as matrix and powders of spherical W and lamellar MoS₂ and B₄C as particulate fillers with different loadings were melt mixed in an internal mixer, followed by compression molding in to sheet form. The goodness of dispersion was manifested via SEM and EDX images. Radiation attenuation capability of these compounds was examined with direct diagnostic x-ray exposure and compared with that of Pb. Dynamic rheology measurements were carried out to evaluate viscoelastic properties of the molten composite materials, necessary in shaping process operations. The mechanical and thermal properties were further investigated from the product performance point of view. Results demonstrated that the flexible composite sheet made with 45% (wt) tungsten provided comparable x-ray absorption to non-flexible lead sheet but much lighter in weight. Significant difference was observed between flow characteristics and yield strength of composite materials of highly loaded spherical metallic particles and lamellar particles of metallic compounds. The melt viscoelastic behavior of former was similar to that of neat matrix melt.

* Corresponding author. Tel.: +98 21-48662421 ; fax: +98 21-44580021-23; E-mail address: j.morshedian@ippi.ac.ir

DOI: 10.22104/jpst.2017.1943.1067

1. Introduction

High energy radiation can be dangerous to human life depending on its energy. The three main rules for protection against the hazards of radiation are time, shielding and distance. Spending the shortest amount of time possible around the radiation source, staying as far away as possible from it, and using a shield between ourselves and the source can reduce the hazardous effects [1, 2]. The intensity of damage depends on the type of radiation, energy of radiation, absorbed dose, exposure time, etc.; unfortunately, the wide range of applications which involved these types of high energy radiation, such as x-ray and gamma-ray, is large. X-ray and gamma-ray are radiation sources found in numerous industries such as aerospace, medical, nuclear reactors, securities and agriculture. Our interest is in the medical industry, particularly radiology, where we are mainly dealing with x-ray and gamma ray. How Since high energy radiations can easily penetrate the human body, high-density materials can be used for radiation shielding [3].

Generally, lead and lead compounds are used for high-energy radiation shielding. However, lead is toxic and aprons are very heavy for personal shielding and also have disposal problems [4]. Therefore, polymer-based composites are particularly interesting candidates as radiation shielding materials for varied reasons such as lightness, environmental-friendliness, non-toxicity and flexibility [5]. Numerous experimental investigations and theoretical studies have reported the use of a variety of shielding materials for attenuation or absorption of undesired radiations, a few of which are mentioned below.

The presence of wolfram metal powder in a styrene-butadiene-styrene copolymer matrix created a new high energy radiation shielding material [6]. In another work, prepared high density polymer-wolfram composites were studied and showed low x-ray transmittance [7].

Another study has been done on the radiation shielding provided by recycled agricultural fiber and industrial plastic wastes with lead oxide and boron carbide produced as composite material. In that study, B₄C was used to absorb the neutron radiation [8].

Moreover, the presence of iodine monobromide

(IBr) in graphite composites showed efficient shielding against x-ray radiation [9], and the presence of CNT has been proven to improve the resistance of PMMA against high-energy radiation [10]. 0.5 weight percentage of single-walled CNT in poly (4-methyl-1-pentene) (PMP) has shown an increase in electromagnetic radiation resistance [11].

It has been seen that concrete containing polystyrene and boron oxide can improve neutron shielding [12]. The presence of borosilicate has been shown to compensate for LDPE weakness of at high temperature and pressure such as that used for shielding in the spacecraft industry [13]. It has been proven that 2 weight percentage of boron nitride in HDPE can improve neutron-beam shielding [14].

Studies have shown that nano-sized boron carbide (B₄C) and boron nitride (BN) powder melt blended with HDPE enhanced thermal neutron attenuation [15].

The purpose of this study is to evaluate whether the developed non-lead polymer composites are effective at blocking diagnostic x-ray radiation. We focused on high-density PE composites containing tungsten, molybdenum disulfide and boron carbide powders separately, and the effect of these particles, mainly on x-ray radiation attenuation, is investigated. The above particulate fillers contain three elements from the 6th and 13th group of the Mendeleev Table, which could be appropriate radiation shields either with a high atomic number or lamellar structure. As the type, structure and size of the filler are important factors in radiation absorption, tungsten metallic powder with its high atomic number and spherical shape, molybdenum disulfide as another high atomic number-metal compound with a lamellar shape, and boron carbide as a compound of a reported effective semi-metal with lamellar shape were chosen to be studied as dispersions in a fiber forming grade high density polyethylene.

Low filled (10%wt) and high filled (45%) composites were prepared by melt blending in an internal mixer. SEM and EDX images were used to study the mixing efficiency method in the blend of particles with HDPE. Radiology pictures and turbidity tests were used for evaluating radiation absorption. For thermal and mechanical properties, DSC and tensile tests were used, respectively. Our other

concern is to know whether the developed composite materials have the potential for use in shaping processes such as extrusion fiber forming, followed by the production of nonwoven fabric or aprons, and compression/injection molding to produce any size, shape and type of shields. In order to achieve this objective it is necessary to study the rheological properties of dispersed systems. Rheology of dispersions of solid particles in polymer melt may be very complex and its control is necessary from a processability point of view [16]. It is worth mentioning that few studies have been made on either radiation absorbance or rheological behavior of the above composite materials.

2. Experimental

The raw materials used in this study consist of HDPE with MFI of 4 gr/10min, tungsten powder with 1.2 μ particle size, boron carbide powder with 10 μ particle size and molybdenum disulfide powder with 5 μ particle size. More information about the material used is mentioned in Table 1.

Table 1. Turbidity of Radiology Images of Lead, HDPE/ 45%(wt) W, HDPE/ 45%(wt) B₄C, HDPE/ 45%(wt) MoS₂

Material	Density (g/cm ³)	Company
HDPE (I4)	0.954	Jam Petrochemical
Boron Carbide	2.5	Pasargad Novin
Tungsten	4.0	Merck
Molybdenum disulfide	5.0	Iran Molybdenum

Samples were prepared in two different 10 and 45 weight percentages for each of the above particles in polyethylene resin. First, HDPE and filler particles with in a specific portion were melt-mixed in an internal mixer (Brabender, Germany) with roller rotors for 4-5 minutes at 190°C at high speed (60 rpm) to obtain a steady torque. Then, the molten mixture was poured into a mold of 2mm thickness at the same temperature and a pressure of 25 bar in the hot press machine. For mechanical, thermal and radiation attenuation tests, primary samples were prepared in the shape of sheets. Scanning electron microscope

(SEM by TESCAN, Czech Republic) equipped with EDX was performed for the compounds morphology. The specimens were broken in liquid nitrogen and the fractured surfaces were coated with gold before taking SEM images at 20 kV and magnification of 150x.

Thermal properties were measured according to ASTM D3418 (by PL-DSC, England). Tensile properties were measured according to ASTM D638 (by Instron, England) for dumbbell shaped specimens. A turbidity test was performed in accordance with ASTM D1003 (by BYK Gardner Haze-gard plus). Dynamic rheological measurements were implemented according to ASTM D4440 (by MCR300, Germany) and melt flow rate measurements were taken according to ASTM D1238 (by Zwick 4100, Germany). Radiology was performed by an X-FRAMES machine, Italy. A gamma ray attenuation test was carried out by two machines, Scintillator and Geiger Muller from ORTEC Company, USA. Irradiation of the samples was conducted at room temperature and in the presence of air. An standard lead specimen of 2.5mm thickness was used as a reference in radiology images taken at x-ray energy intensities of 40 and 80 Kev.

3. Results and discussion

The morphology of compounds characterized by SEM is presented in Figures 1a to 1f. These images also show the dispersed particle size. Figures 1e and 1f reveal the lamellar structure for molybdenum disulfide with a particle size of 5 μ m to 15 μ m particle size. It is observed that the dispersion of 45% (wt) molybdenum disulfide in the HDPE matrix is not quite uniform due to the rather high interaction of these particles with each other, hence only a few agglomerations have formed. Figures 1a and 1b show the lamellar structure of boron carbide particles 10 μ m to 20 μ m in particle size. SEM images for tungsten compounds in Figures 1c and 1d show a spherical structure of particles of 1.2 μ m to 2 μ m in size. Both tungsten and boron carbide have uniform dispersion and distribution in the matrix according to the SEM and EDX results. EDX images in Figures 2a to 2f show the efficiency of the mixing method and a good distribution of mineral particles in the HDPE matrix.

The backscatter application was used for the EDX

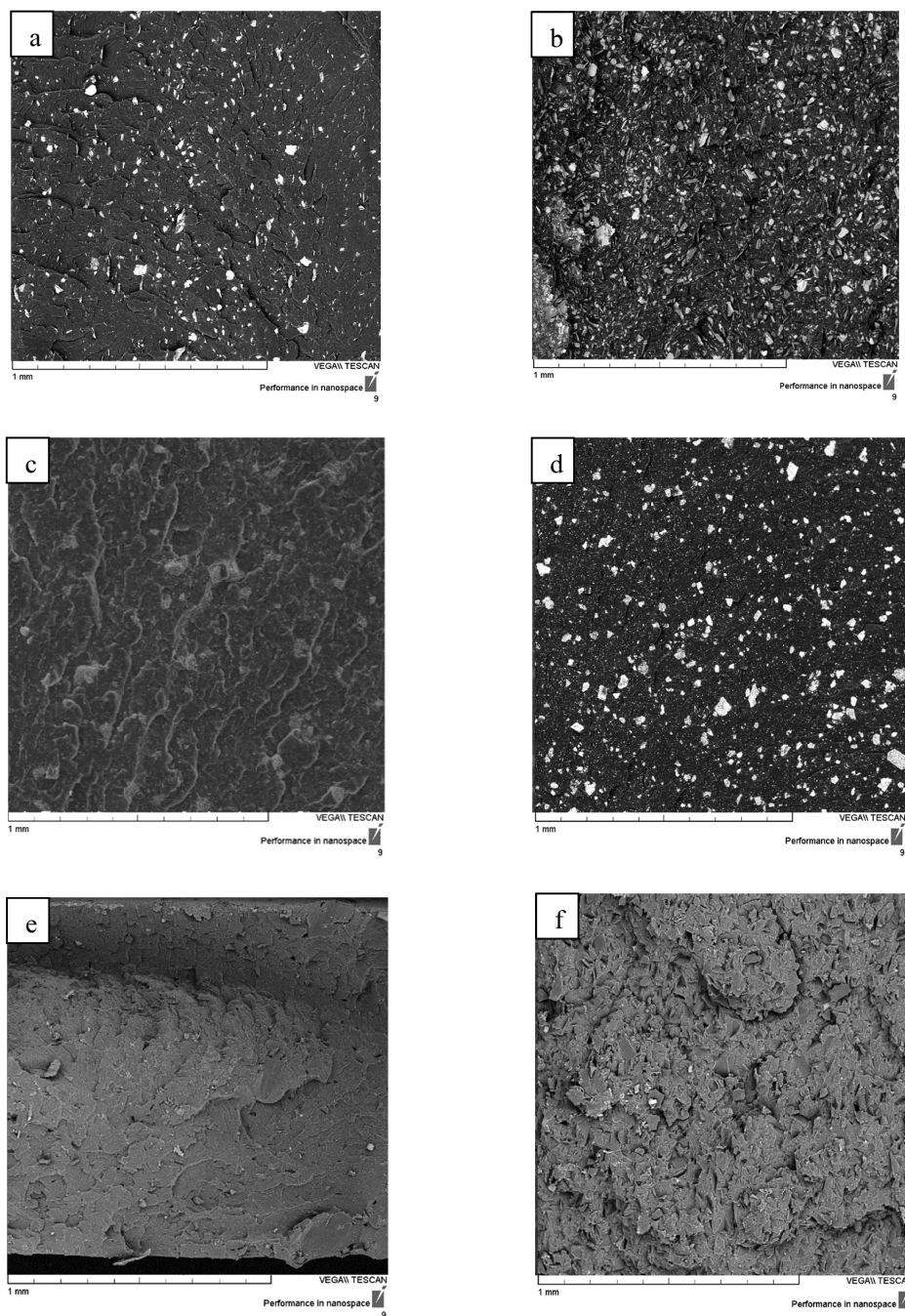


Fig. 1. SEM images HDPE/ a) 10%(wt) B_4C , b) 45%(wt) B_4C , c) 10%(wt) W, d) 45%(wt) W, e) 10%(wt) MoS_2 , and f) 45%(wt) MoS_2 .

images. This application is only used for mineral particles and shows these particles bolder and more visible in the matrix.

Figures 3a and 3b are the images of the x-rays exposure on 2mm thick composite sheets containing 10 and 45% (wt) of particulate fillers and a neat lead sheet of 2.5mm thickness. A digital radiology machine is used for investigating the x-ray

transmittance through the samples at two different energy intensities 40 and 80 KeV, which are common energy intensities used in radiology. The lighter the image is, the more x-ray absorption has occurred. As it is observed from the radiology images, the HDPE/ 45% (wt) tungsten has x-ray attenuation comparable to that of the neat lead. A turbidity test was used to allow for a quantitative comparison. The turbidity

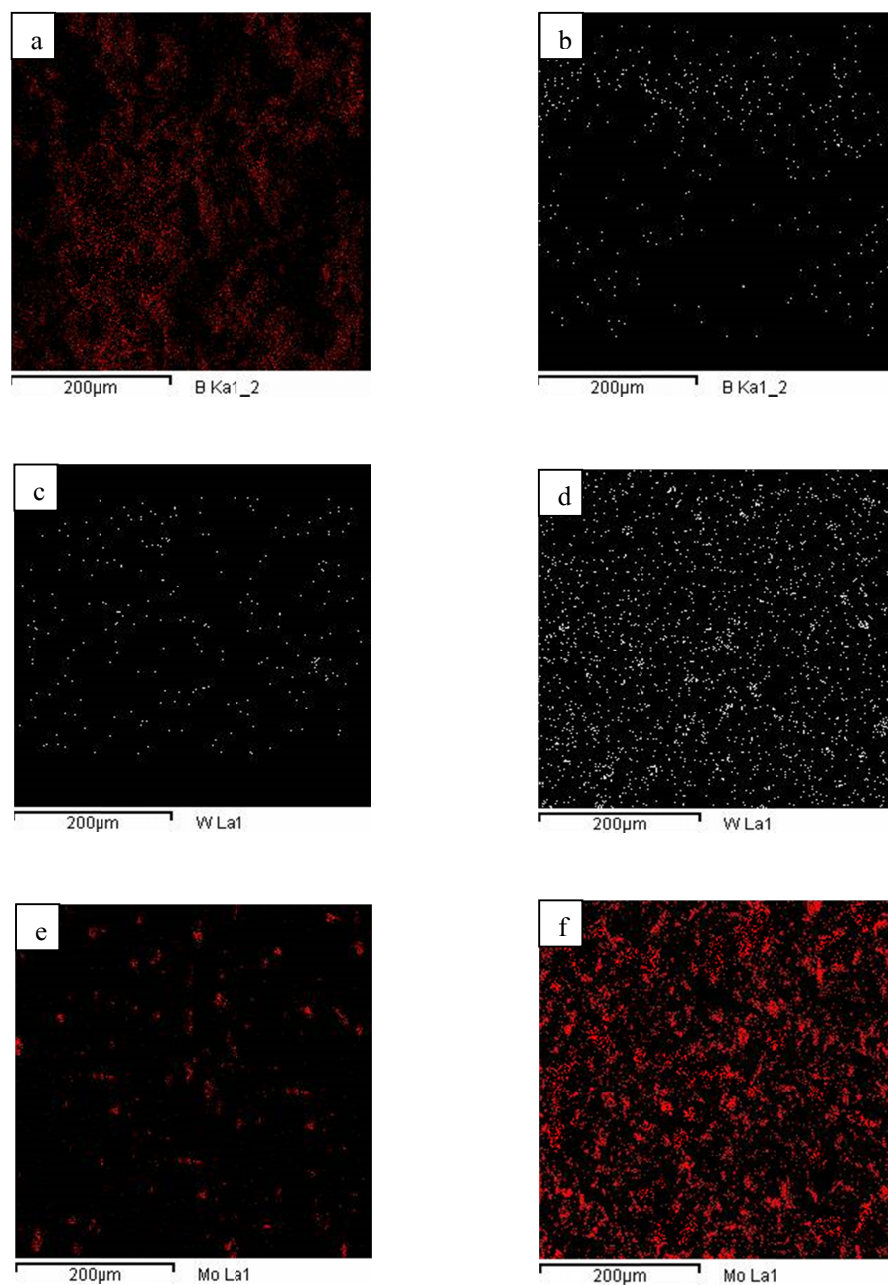


Fig. 2. EDX images HDPE/ a) 10%(wt) B₄C, b) 45%(wt) B₄C, c) 10%(wt) W, d) 45%(wt) W, e) 10%(wt) MoS₂, and f) 45%(wt) MoS₂.

result is given in Table 1. As the numbers show, the polyethylene composite containing 45% (wt) tungsten has almost a similar turbidity to that of lead, although the sample thicknesses are different. Assuming a linear relationship between thickness and absorption (as learned from GM results), almost an identical turbidity is obtained for the same thickness of 45% (wt) W sample and lead. The other point achieved by these results is that varying the radiation intensity

does not change the order of x-ray absorption values by the samples, and in all intensities used the best absorption was achieved by HDPE/45% (wt) tungsten. The overall conclusion on X-ray results are: i) A high atomic number is the most important parameter in radiation attenuation, ii) particle packing is another important influencing factor, and iii) at comparable atomic numbers and packing factor, particles with lamellar shape are more effective than spherical



Fig. 3. Radiology images at intensities of a) 40 and b) 80 KeV x-ray for neat lead, 10 and 45 % (wt) of boron carbide, tungsten and molybdenum disulfide in HDPE.

particles, for instance at 10% loadings where MoS_2 lamellar shaped particles are well dispersed in the HDPE matrix; they demonstrate better barrierity against x-ray radiation

It must be noted that the effective x-ray absorption of some of these composite materials holds against their much lower density compared to that of lead, which greatly influences the weight of products, such as apron, made of them. Table 2 shows the result of density measurements on lead, neat HDPE and its composites.

Table 2. Density of Lead, Neat HDPE and its Composites

Samples	Density (g/cm^3) (± 0.005)
Lead	11.34
HDPE	0.95
HDPE/45%(wt) W	1.48
HDPE/45%(wt) MoS_2	1.54
HDPE/45%(wt) B_4C	1.26

To investigate gamma ray attenuation through the samples, we used a Geiger Muller Counter (GM) and a 3"×3" scintillation spectroscopy detector both with Co_{60} gamma-ray source. As shown in the x-ray results, only the samples consisting of 45% (wt) of tungsten, boron carbide and molybdenum disulfide in HDPE with a 2 mm thickness and 3 cm distance from the detector were tested. One the ends of the detector is made of a thin mica window that allows passage of beta particles and low energy gamma radiations which would otherwise be stopped by the metal cover provided for detection of gamma radiations. The number of outgoing rays from the source and the number of passing through radiation from the samples are counted by this machine. In this way the number of absorbed rays was obtained according to equation (1).

$$\text{Absorption percentage} = (C_0 - C)/C_0 \quad (1)$$

In this equation, C_0 is the number of primary rays and C is the number of passing through rays.

The results of this test, as the number of passing through rays for samples with 2mm and 4mm thicknesses, are shown in Table 3. The exposure time was 100 seconds.

Table 3. Number of passing through Rays in Geiger Muller Test for Samples with 2mm and 4mm Thicknesses

Sample	Number of passing through rays	
Source(Cs)	4	
Thickness	2mm	4mm
HDPE	3995	3994
HDPE/45%(wt) W	3887	3767
HDPE/45%(wt) MoS_2	3927	3855
HDPE/45%(wt) B_4C	3935	3887

According to data from Table 3, doubling the thickness of the samples nearly doubled the absorption percentage obtained from equation 1. According to Table 3, HDPE/45% (wt) tungsten had more absorption than HDPE/45% (wt) boron carbide and HDPE/45% (wt) molybdenum disulfide. The number of passing through rays for neat lead was 3330.

Table 4 shows the result of Scintillator with a Co source for neat HDPE and its composites. According

to this table, the best result was attained for HDPE/45% (wt). This is due to the high atomic number of tungsten, which has great influence on the absorption ability of this compound.

Table 4. Scintillator Result with Co Source for Neat HDPE, HDPE/45%(wt) tungsten, HDPE/45%(wt) boron carbide, HDPE/45%(wt) molybdenum disulfide

Sample	Time (s)	Number of passing through rays
HDPE	200	551732
HDPE/45%(wt) W	200	477741
HDPE/45%(wt)MoS ₂	200	492514
HDPE/45%(wt)B ₄ C	200	538670

Figures 4 and 5 are spectrum plots of gamma-ray detector data (Co source) for neat HDPE and HDPE/45% (wt) W, respectively. The spectrum plots of B₄C and MoS₂ composites are similar to the spectrum plot of tungsten composite and available in Figures 6 and figure 7, respectively. The vertical axis shows the number of passing through rays and the horizontal axis shows the number of channels. The first peak in all plots is the backscatter peak, and the region between the backscatter and the main peak (which is the highest one and shows the number of passing through rays) is the Compton region. The 45%wt tungsten loading in HDPE exhibited greater photon efficiency than 45%wt loading of MoS₂ or B₄C, which would allow for greater gamma-ray attenuation and thus greater photon protection.

ATR analysis on samples exposed to gamma-ray in a Scintillator machine was used to investigate the radiation degradation of HDPE/45% (wt) W due to its gamma ray absorption ability. Figure 8 shows the ATR spectrum for neat HDPE before and after exposure to gamma-ray radiation; it shows two extra peaks at 1243cm⁻¹ and 1158cm⁻¹ wavenumber due to the formation of double bonds after exposure of the resin to gamma radiation. These double bonds belong to terminal vinyl groups generated due to chain scission degradation of HDPE.

Figure 9 shows the ATR spectrum of HDPE/45% (wt) tungsten before and after exposure to gamma-ray radiation. As it is clear from the graph, no change has appeared in the polymer chemical structure after radiation. So dispersion of tungsten powders in the

HDPE matrix brings about stability to polyolefin against gamma ray radiation.

Comparing ATR spectrums of neat HDPE and irradiated HDPE shows the appearance of two peaks at 1158 cm⁻¹ and 1243 cm⁻¹ after gamma radiation, which are assigned to creation ethers and esters groups due to oxidative degradation. All other peaks are due to different CH₂ and CH₃ absorptions.

For studying HDPE's flow behavior containing different particles, small amplitude oscillating shear measurements were conducted on polyethylene samples loaded with 10 and 45 weight percentages of particulate fillers at 200°C. Figure 10 shows the complex viscosity of these samples against frequency. It is revealed that the resistance to flow of HDPE filled with lamellar particles, particularly MoS₂, is much higher than the neat resin as well as the resin filled with spherical tungsten powders. The viscosity rise of MoS₂ samples to very high values at low frequency, as observed in their SEM images, is due to the presence of agglomerates as well as possible formation of a weak gel-network by bridging flocculation. The intensive shear thinning of these samples indicates disagglomeration and break down of gel-network structure upon shearing. As it is shown in Figure 10, neat HDPE, HDPE/10% (wt) tungsten and HDPE/45% (wt) tungsten curves have the same slope. This means that no difference appears between loaded system and non-loaded system behavior when by the frequency of oscillations or shear intensity increases. This phenomenon shows that the dispersion of these particles in the matrix was good enough and no more dispersion occurred by increasing the shear rate and only disentanglement and chain orientation happen as shear increased. Similar flow behavior of tungsten filled samples to that of neat HDPE is very interesting and shows only a few interactions of tungsten particles with their surroundings occur as they roll over and are displaced in the shear field. For hard-sphere dispersions, where both repulsion and attraction are screened, the rheological behavior is simple and it depends only on the balance between Brownian diffusion and hydrodynamic interactions. However, we may compare the observed behavior with the prediction of Einstein's theory for suspension of rigid, non-interacting spherical particles in Newtonian fluids:

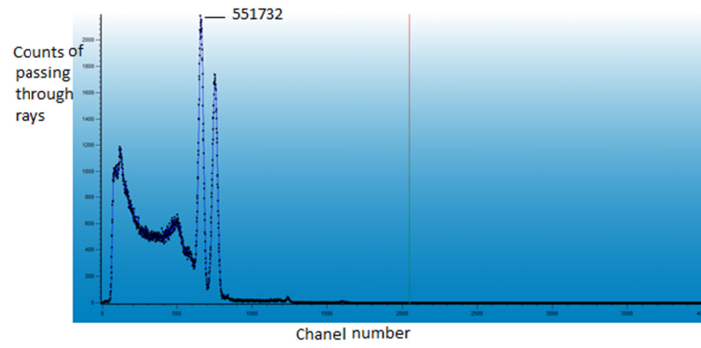


Fig. 4. Spectrum of neat HDPE by Scintillator with Co source.

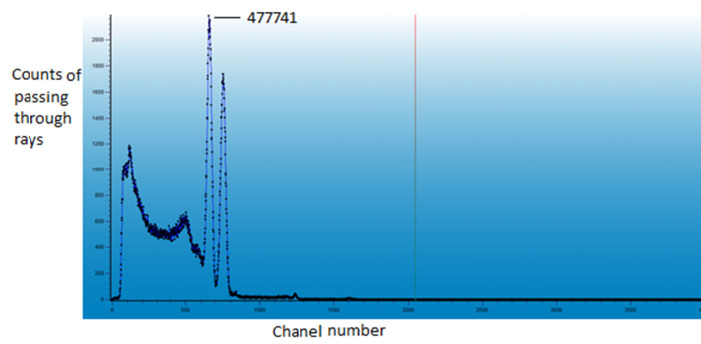


Fig. 5. Spectrum of HDPE/45% (wt) tungsten by Scintillator with Co source.

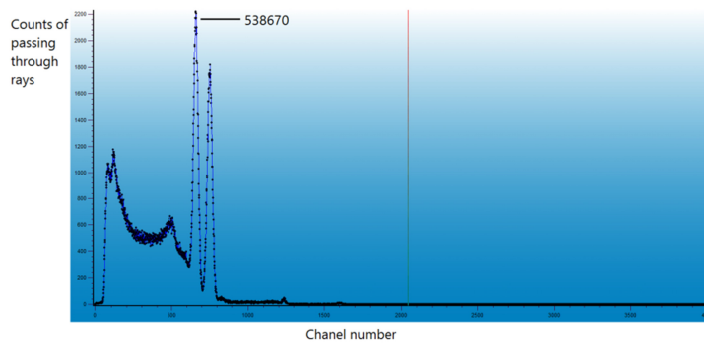


Fig. 6. Spectrum of HDPE/45% (wt) B₄C by Scintillator with Co source.

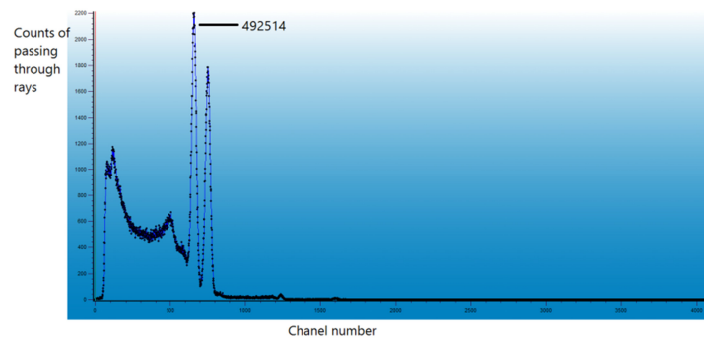


Fig. 7. Spectrum of HDPE/45% (wt) MoS₂ by Scintillator with Co source.

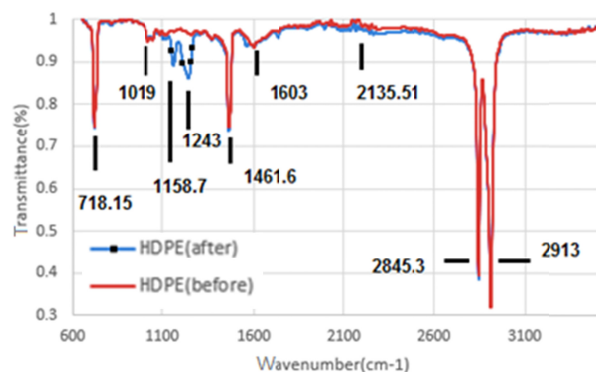


Fig. 8. ATR spectrum of HDPE before and after gamma irradiation by Scintillator machine.

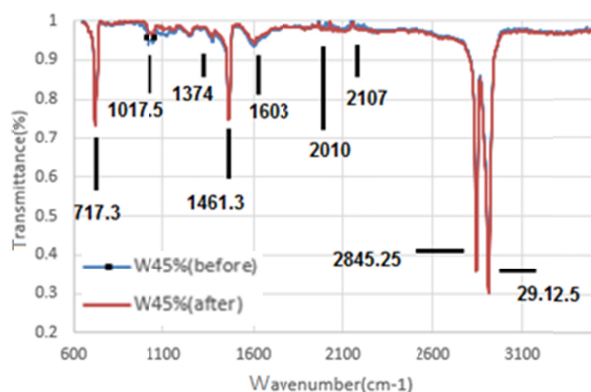


Fig. 9. ATR spectrum of HDPE/45%(wt) W before and after gamma irradiation by Scintillator machine.

$$\eta = \eta_0 (1 + 2.5\phi) \quad (2)$$

In this equation, η and η_0 are the mixture and matrix viscosity at near-zero shear rates, respectively, and ϕ is the volume fraction of particles. The ratio of η to η_0 for HDPE/45% (wt) tungsten in this rheology test was 1.11 and this ratio from Einstein's prediction for this compound was 1.07. So, with this very good approximation it is possible to state that this sample has obeyed this theory even though the liquid resin is not Newtonian. This phenomenon shows that rigid tungsten particles had no interaction with the PE matrix and hydrodynamic effects were negligible. So the tungsten particles slipped in the matrix and had no hydrodynamic effects on themselves. Although Einstein equation stands for small amounts of filler in suspension, it was shown that even for 45%wt tungsten in molten HDPE, due to very good dispersion/distribution and no particle-particle or particle-polymer interaction, deviation of the mixture behavior from equation 2 is small. This was the main

difference of tungsten particles and other particles used in HDPE matrix rheology. Mind that the SEM images revealed that the particle size of tungsten powder in the compound was the same as the received sample. Measurement of the melt flow index at 190c under load of 2.16kg confirmed the above rheological result. So that the MFI for neat HDPE was 4.0 gr/10 min, and that for HDPE/45% (wt) W was 3.9 gr/10 min. As a result we do not have to cope with increased viscosity of the melt due to the incorporation of high amounts of W powder, which is a great advantage in the processability of this system.

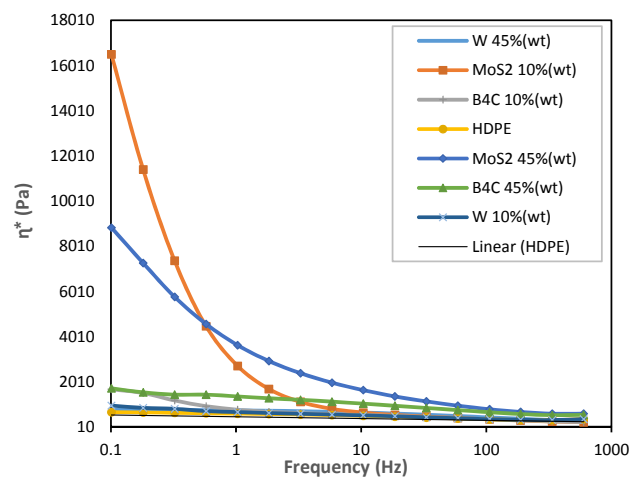


Fig. 10. Complex viscosity curves vs frequency at 200°C.

Figure 11 shows storage modulus, G' , as an indication of elasticity of different samples versus frequency at 200°C. In agreement with SEM images and viscosity curves, it is seen that HDPE/45% (wt) molybdenum disulfide has the highest elasticity and a modest slope of increase with frequency due to the agglomerated and gel-formed lamellar structure of the particles in the matrix. The low frequency, nearly flat part seen in the curve of this sample in Figure 11 together with the high initial viscosity in Figure 10 indicate that this compound has a semi solid-like elastic behavior with a semi-yield stress in melt state. The other curves demonstrate almost linear viscoelastic behavior in the low frequency region. Furthermore, addition of tungsten powders has little effect on the curve of the neat molten HDPE, indicating little elastic improvement with the addition of these metal particles to the resin. Figure 12 shows loss modulus, G'' , curves of the samples versus frequency at 200°C. While the MoS_2 filled sample had

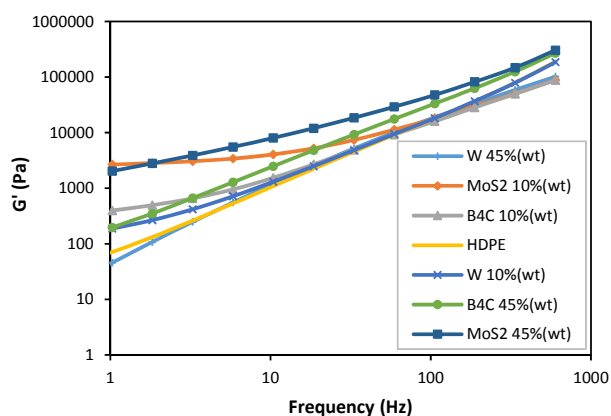


Fig. 11. Storage modulus curves vs frequency at 200°C.

the highest elasticity, it manifested the highest dissipation of energy due to the structure build-up mentioned above. As with η_3^* and G' curves, G'' curves of neat HDPE and tungsten filled resin coincide almost on each other, meaning that the HDPE/tungsten compound has the same elastic and viscose effects as the neat resin has in its melt processing.

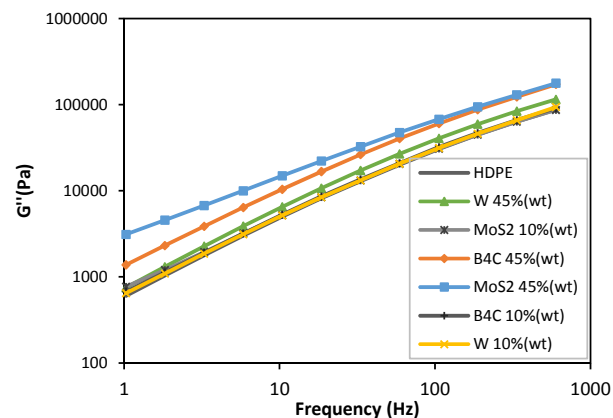


Fig. 12. Loss modulus curves vs frequency at 200°C.

Since the aim of this study was to prepare a lead replacement for radiation shielding and only the compounds containing 45% (wt) particles were relatively suitable according to the radiology images, other tests such as tensile and thermal analysis were conducted only on this ratio of loaded samples in further investigations.

Tensile tests were employed to evaluate the mechanical properties. Figure 13 shows a comparison of the bar chart of the yield strength, yield strain and modulus of neat HDPE with those of the prepared

composites, and Table 5 shows the same properties with their exact values. It is seen that incorporating 45% (wt) tungsten powder in HDPE improves the tensile properties, contrary to the effect of other particles. The main and bold point here is that this sample has a higher yield strength and strain than neat HDPE. Higher yield strength and stiffness (modulus) imply greater shape resistance against mechanical loading. With 45% (wt) tungsten loading, the composite material still yields, even at higher strain, and has ductile and flexible behavior at room temperature. It is anticipated at large weight fractions, such as 45% where W metal particles separation distances are small, they attract each other by van der Waals forces. This attraction energy is eliminated at high temperature, in the melt state.

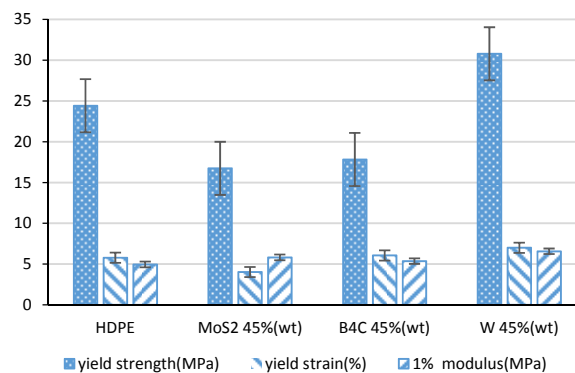


Fig. 13. Tensile bar chart of HDPE and its prepared composites.

DSC test was employed to examine the thermal properties of samples containing 45% (wt) fillers. Cooling and heating curves in the DSC test are shown in Figures 14 and 15. The degree of crystallinity (X_c) was calculated based on the crystallization enthalpy ΔH_c values from Figure 15. The crystallization enthalpy of 100% crystalline PE (ΔH_c^0) was found to be 288J/gr [17]. Table 6 demonstrates the thermal properties as the melting temperature, crystallinity percentage and crystallization temperature of neat HDPE and 45% (wt) filler loaded compounds. From these data it was understood that the presence of these fillers in the polymer matrix did not change the melting temperature and crystallinity of HDPE. In other words, these particles neither act as a nucleating agent nor bring about any disturbances for crystal formation of molten matrix upon cooling.

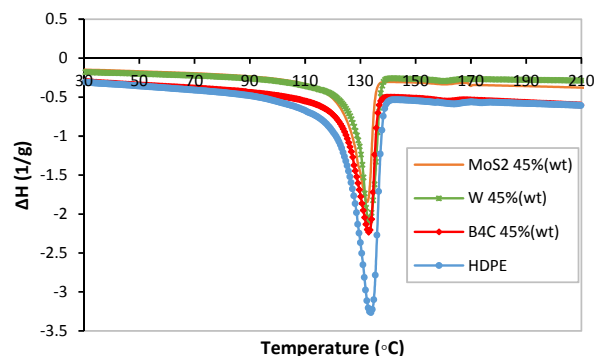


Fig. 14. Heating DSC curves for composite samples containing 45% (wt) fillers at a temperature range of 50 to 200°C.

Furthermore, as it is observed from Figure 15 and Table 6, adding B₄C and MoS₂ particles to polyethylene increases the crystallization temperature (T_c) because of their lamellar structure and their higher thermal conductivity. As a result, the cooling/solidifying time or molding cycle in injection molding operation is shortened.

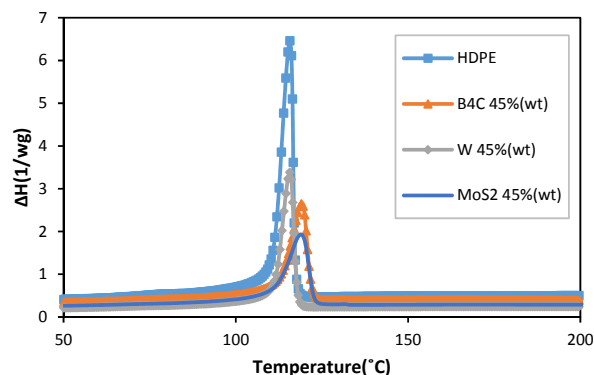


Fig. 15. Cooling DSC curves for composite samples containing 45% (wt) fillers at a temperature range of 50 to 200°C.

4. Conclusion

Developed low density 45% (wt) tungsten powder loaded high density polyethylene composite material demonstrates nearly equivalent x-ray radiation attenuation with an energy intensity of up to 80KeV used in radiology compared to toxic high density Pb-based material [18][3]. While this composite material also provides good shielding protection against higher energy, γ -ray radiation emitted from Co₆₀ source in Scintillator machine, the absorbed radiation dose did not change the chemical structure of the polyolefin matrix, contrary to its degradative effect on unloaded neat resin.

Interparticle interaction within lamellar MoS₂ particles dispersed in molten HDPE causes the formation of a weak gel-network structure with solid-like behavior and yield stress in shear flow. In quenching under quiescent condition, the crystallization temperature of matrix shifts to a higher temperature implying shortening of the cooling/solidifying time. In contrast, even high loadings of spherical tungsten powder not only does not alter the thermal properties of polymer phase, likewise, it hardly modifies the viscoelastic shear flow characteristics of neat base HDPE resin, implying the same ease of processing as the neat matrix is preserved in the composite material. Nevertheless, in solid state, 45% (wt) tungsten filled composite still has ductile and flexible behavior, enjoying higher yield strength and strain and stiffness than neat HDPE.

Table 5. Tensile Test Results

Test	HDPE	HDPE/45% (wt) MoS ₂	HDPE/45% (wt) B ₄ C	HDPE/45% (wt) W
Yield strength (MPa)	24.4	16.7	17.8	30.8
Yield strain (%)	5.8	4.0	6.0	7.0
1% Modulus (MPa)	4.9	5.8	5.4	6.6

Table 6. Some Thermal Properties of Samples.

Sample	Crystallinity percentage (%)	Crystallization temperature, T_c , (°C)	Melting point (°C)
HDPE	63.0	115.69	133.96
HDPE/45% (wt) W	62.2	115.63	133.08
HDPE/45% (wt) B ₄ C	64.5	119.02	133.20
HDPE/45% (wt) MoS ₂	63.0	118.88	132.46

References

- [1] X. Cao, X. Xue, T. Jiang, Z. Li, Y. Ding, H. Yang, Mechanical properties of UHMWPE/Sm₂O₃ composite shielding material, *J. Rare Earth.*, 28 (2010) 482-484.
- [2] S. Navas, Study of the neutron shielding capacity of different carbon materials for space application, Dep. Space Programs and Sciences, National Institute of Aerospace Technology. (2016).
- [3] S. Nambiar, J.T. Yeow, Polymer-composite materials for radiation protection, *ACS Appl. Mater. Inter.*, 4 (2012) 5717-5726.
- [4] A. Bhattacharya, Radiation, industrial polymers, *Prog. Polym. Sci.*, 25 (2000) 371-401.
- [5] C. Harrison, S. Weaver, C. Bertelsen, E. Burgett, E. Grulke, Polyethylene/boron nitride composites for space radiation shielding, *J. Appl. Poly. Sci.*, 109 (2008) 2529-2538.
- [6] K. Yue, W. Luo, X. Dong, C. Wang, G. Wu, M. Jiang, A new lead-free radiation shielding material for radiotherapy, *Radiat. Prot. Dosim.*, 133 (2009) 256-260.
- [7] T. Ivanoua, K. Bliznakova, N. Pallikarakis, Simulation studies of field shaping in rotational radiation therapy, *J. Med. Phys.*, 33 (2006) 4289-4298.
- [8] A. El-Sayed Abdo, M.A.M. Ali, M.R. Ismail, Natural fiber high-density polyethylene and lead oxide composites for radiation shielding, *Radiat. Phys. Chem.*, 66 (2003) 185-195.
- [9] J.R. Gaier, W. Hardebeck, J.R.T. Bunch, M.L. Davidson, D.B. Beery, Effect of interaction in graphite epoxy composites on the shielding of high energy radiation, National aeronautics and space administration, Washington, D.C., 1997.
- [10] E. Najafi, K. Shin, Radiation resistance polymer-carbon nanotube nanocomposite thin films, *Colloid. Surface. A*, 257-258 (2005), 333-337.
- [11] L.M. Clayton, T.G. Gerasimor, M. Cinke, M. Meyyappan, J.P. Harmon, Dispersion of Single-Walled Carbon Nanotubes in a Non-Polar Polymer, Poly(4-methyl-1-pentene), *J. Nanosci. Nanotechno.*, 6 (2006) 2520-2524.
- [12] G. Gnduz, A. Usanmaz, A development of new nuclear shielding materials containing vitrified colemanite and impregnated polymer, *J. Nucl. Mater.*, 140 (1986) 4-55.
- [13] M.M. Ashton-Patton, M.M. Hall, J.E. Shelby, Formation of low density polyethylene/ hollow glass microspheres composites, *J. Non-Cryst. Solids*, 352 (2006) 615-619.
- [14] C. Harrison, S. Weaver, C. Bertelsen, E. Burgett, N. Hertel, Radiation Oncology Physics, Polyethylene/boron nitride composites for space radiation shielding, *J. Appl. Polym. Sci.*, 109 (2008) 2529-2538.
- [15] J. Kim, B. Lee, Y. Rang, Enhancement of thermal neutron attenuation of nano-B₄C, -Bn dispersed neutron shielding polymer composites, *J. Nucl. Mater.*, 453 (2014) 48-53.
- [16] T.F. Tadros, *Rheology of Dispersions: Principles and Applications*, Wiley-Vch, New York, 2010.
- [17] F.M. Mirabella, A. Bafna, Determination of the crystallinity of polyethylene/ α -olefin copolymers by thermal analysis: Relationship of the heat of fusion of 100% polyethylene crystal and the density, *J. Polym. Sci.*, 15 (2002) 1637-1643.
- [18] Y. Kim, S. Park, Y. Seo, Enhanced X-ray shielding ability of polymer-nonleaded metal composites by multilayer structuring, *Ind. Eng. Chem. Res.*, 54 (2015) 5968-5973.